A unified approach to the dynamics of a polymer melt

2006 J. Phys.: Condens. Matter 18 S2391

(http://iopscience.iop.org/0953-8984/18/36/S13)

INSTITUTE OF PHYSICS PUBLISHING JOURNAL OF PHYSICS: CONDENSED MATTER

J. Phys.: Condens. Matter **18** (2006) S2391–S2402 doi:10.1088/0953-8984/18/36/S13

A unified approach to the dynamics of a polymer melt

Jean-Marc Zanotti[1,2], Luis J Smith[2], David L Price[2,3] and Marie-Louise Saboungi[4]

[1] Laboratoire Léon Brillouin (CEA-CNRS), CEA Saclay, 91191 Gif/Yvette cedex, France
[2] Argonne National Laboratory, Argonne, IL 60439, USA
[3] CRMHT, 1d ave de la Recherche Scientifique, 45071 Orléans cedex 2, France
[4] CRMD, 1b rue de la Ferollerie, 45071 Orléans cedex 2, France

Received 8 February 2006
Published 24 August 2006
Online at stacks.iop.org/JPhysCM/18/S2391

Abstract

Stretched exponentials are often used to describe quasi-elastic neutron scattering (QENS) and nuclear magnetic resonance (NMR) relaxation data from polymer melts. In this paper, we attempt to derive a more physically meaningful model of the local (∼0.1 nm), short-time (∼10 ps) dynamics of linear polymers that takes into account (i) orientational diffusion along the polymer chain, (ii) local conformational transitions, and (iii) long-time, large-scale motions. The model takes into account the spatial component of the local dynamics, described in terms of the scattering vector Q. The model is applied to QENS results on highly entangled polyethylene oxide (PEO) melt at 373 K. We find the Q dependences of the three correlation times of the model to be consistent with Q^0, Q^{-2} and Q^{-4} power laws, respectively. The high-Q limit of the model closely resembles the NMR-based DLM model (Dejean de la Batie *et al* 1988 *Macromolecules* **21** 2045) but the physical interpretation is different. At 373 K, the polymer dynamics is described in terms of transverse motions of the chain segments over a distance of a few nm, with a local monomeric diffusion coefficient of 1.78×10^{-9} m^2 s^{-1}. From this value, we derive a monomeric friction coefficient $\xi_0 = 2.89 \times 10^{-12}$ N s m^{-1} that, used as numerical input to the Doi–Edwards theory, leads to a chain centre-of-mass diffusion coefficient $D_{cm} = 9.4 \times 10^{-15}$ m^2 s^{-1}. This value is in good agreement with pulsed field gradient NMR data (Appel and Fleischer 1993 *Macromolecules* **26** 5520) and validates the proposed model.

(Some figures in this article are in colour only in the electronic version)

1. Introduction

Certain macroscopic properties of polymers, for example the molecular-weight dependence of the viscosity, follow universal power laws [1]. Over the last 50 years, a large body of

theoretical and experimental work has been devoted to the microscopic dynamical origins of such behaviour.

The Rouse model [2] has been used successfully to describe the physics of short-chain polymer melts. This model ignores the atomic structure and treats the coarse-grained structure as a linear succession of beads that interact through a harmonic potential. The conformational entropy is the restoring force that prevents large excursions from equilibrium. For long chains (high molecular-weight polymers), the presence of entanglements leads to the well-known reptation mechanism [3] in which, due to strong inter-chain interactions, the motion of a particular chain is constrained within an imaginary tube formed by the surrounding matrix and defined by the overall contour of the chain under consideration. At short times, the chain experiences the classical Rouse dynamics until the root-mean-square displacements reach the characteristic diameter of the tube, causing a crossover to the reptation regime at longer times.

Among several experimental approaches used to probe polymer dynamics, significant progress has been achieved with nuclear magnetic resonance (NMR) [4] and quasi-elastic neutron scattering (QENS) [5]. QENS measurements suggested that, even at short times and distances, i.e. for values of the scattering vector Q above 0.2–0.3 Å^{-1}, the Rouse model fails to describe the local dynamics, due either to local polymer stiffness [6] or to intra-chain friction related to local conformational changes [5]. At higher Q s, the intermediate scattering functions $I(Q, t)$ have been represented successfully by stretched exponentials [7, 8]. Despite significant deviations from the ideal form of the Rouse model and a lack of clear physical significance, this approach has provided a useful link between the short-time/high-Q and long-time/low-Q regimes.

In this paper, we attempt to derive a more physically meaningful model of the local ($\sim$0.1 nm), short-time ($\sim$10 ps) dynamics of linear polymers that takes into consideration (i) orientational diffusion along the polymer chain, (ii) local conformational transitions, and (iii) long-time, large-scale motions. The model takes into account the spatial component of the local dynamics, described in terms of the scattering vector Q. The model is applied to QENS results on highly entangled polyethylene oxide (PEO) melt at 373 K.

2. Dynamical model

This section provides a derivation of the incoherent dynamical structure factors measured in QENS, arising from the various types of motion that come into play in a polymer chain.

2.1. General formalism

In the case of hydrogenous liquid samples that scatter mainly incoherently, QENS measures the incoherent scattering function $S_{\text{inc}}(Q, \omega)$, the Fourier transform over space and time of the self-correlation function $G_{\text{s}}(r, t)$ of the nuclei in the system. If these particles do not experience perfectly ergodic dynamics, $G_{\text{s}}(r, t = \infty)$ is non-zero. In that case, $S_{\text{inc}}(Q, \omega)$ contains an elastic component and takes the general form [9]

$$S_{\text{inc}}(Q, \omega) = \frac{1}{\pi} \int \int G_{\text{s}}(r, t) \mathrm{e}^{\mathrm{i}Qr - \omega t} \, \mathrm{d}r \, \mathrm{d}t = A(Q)\delta(\omega) + (1 - A(Q)) \, D(Q, \omega) \tag{1}$$

where $D(Q, \omega)$ is related to the time dependence of the particle autocorrelation function. This term is generally described by a sum of Lorentzian lines [9] and in practice is often well represented by a single Lorentzian of half-width half-maximum (HWHM) $\tau(Q)^{-1}$:

$$D(Q, \omega) \approx L(Q, \omega) = \frac{1}{\pi} \frac{\tau(Q)^{-1}}{\tau(Q)^{-2} + \omega^2}. \tag{2}$$

The elastic incoherent structure factor (EISF) $A(Q)$ is the Fourier transform of the $G_s(r, t = \infty)$ loci. In the case of a particle diffusing inside a confining volume, such as a sphere or cylinder, $A(Q)$ is the form factor of this volume. This formalism can also describe other motions such as polymer conformational changes: for a particle experiencing reorientational dynamics between two distinct sites separated by a distance d_j, after orientational averaging (since we are dealing with isotropic samples), the EISF is given by

$$A_{\text{jump2sites}}(Q) = \frac{1 + j_0(Qd_j)}{2} \tag{3}$$

where j_0 is the zeroth-order spherical Bessel function of the first kind.

2.2. Local conformational transitions

If the conformational motions experienced by a monomer are characterized by a single correlation time τ_0, the corresponding scattering function is

$$S_{\text{inc}}^{\text{Conf}}(Q, \omega) = A_0(Q)\delta(\omega) + \frac{1 - A_0(Q)}{\pi} L^{\text{Conf}}(Q, \omega) \tag{4}$$

where $L^{\text{Conf}}(Q, \omega)$ is a Lorentzian function with HWHM $\tau_0(Q)^{-1}$ and $A_0(Q)$ is the EISF associated with the geometry of the motion.

2.3. Orientational diffusion along the polymer chain

In the case of crystalline PEO, two-dimensional (2D) ^{13}C solid-state NMR experiments have shown [4] that the conformational transitions can be described as helical jump (HJ) motions. This process, which is very slow at 225 K, involves a rotation of a given monomer by 180° with a concomitant chain translation of one monomer unit. This translation can be described as a random walk in continuous time (RWCT), a generalization of the discrete random walk in which the waiting time probability density is no longer a Dirac function but has a time dependence $\Psi(t)$. If $\Psi(t)$ is Poissonian, which is the case for conformational changes in PEO melt [10], the autocorrelation function of the motion is given by

$$G^{\text{HJ}}(t) = \mathrm{e}^{-t/\tau_1} I_0(t/\tau_1) \tag{5}$$

where τ_1^{-1} is the rate of the conformational changes and I_0 is the zeroth-order modified Bessel function of the first kind.

The long time scales over which HJ motions takes place at 225 K are inaccessible with QENS, but we can expect these motions to be still present above the melting point but several orders of magnitudes faster and thus within the dynamical range of QENS. It should be noted however that, due to the combined effect of damping originating from the averaged dynamics of the neighbouring chains and of the presence of entanglements, the diffusion of the polymer chains implied by the HJ motions should not extend beyond a few nm. These localized diffusive motions give rise to a scattering function

$$S_{\text{inc}}^{\text{Diff}}(Q, \omega) = A_1(Q)\delta(\omega) + \frac{1 - A_1(Q)}{\pi} S_{\text{inc}}^{\text{HJ}}(Q, \omega) \tag{6}$$

where $A_1(Q)$ is the form factor of the volume over which the diffusion takes place and $S_{\text{inc}}^{\text{HJ}}(Q, \omega)$ is the Fourier transform of equation (5) with τ_1 now taken to be Q-dependent.

2.4. Long-time, large-scale motions

At times beyond those where this atomic description applies, larger-scale polymer viscoelastic properties have to be taken into account. The present work focuses on high Q (>0.36 Å) data

in which these larger-scale motions are not likely to be described accurately. For the present purposes, they will be accounted for by a single relaxation time $\tau_2(Q)$, leading to the scattering function

$$S_{\rm inc}^{\rm Glob}(Q,\omega) = \frac{1}{\pi}\int \mathrm{e}^{-t/\tau_2}\mathrm{e}^{\mathrm{i}Qr-\omega t}\,\mathrm{d}t. \tag{7}$$

2.5. Total incoherent dynamical structure factor

Assuming that the different dynamical mechanisms described in Sections 2.2 through 2.4 are uncorrelated, the final scattering function $S_{\rm inc}^{\rm PEO}(Q,\omega)$ describing the PEO dynamics is a convolution of equations (4), (6) and (7). The correlation time τ_0 representing the local reorientational dynamics is expected to be much shorter than τ_1 and τ_2 so that, to a good approximation,

$$L^{\rm Conf}(Q,\omega)\otimes S_{\rm inc}^{\rm HJ}(Q,\omega) \approx L^{\rm Conf}(Q,\omega) \tag{8}$$

$$L^{\rm Conf}(Q,\omega)\otimes S_{\rm inc}^{\rm Glob}(Q,\omega) \approx L^{\rm Conf}(Q,\omega) \tag{9}$$

and $S_{\rm inc}^{\rm PEO}(Q,\omega)$ becomes

$$\begin{aligned} S_{\rm inc}^{\rm PEO}(Q,\omega) = {} & A_0(Q)A_1(Q)S_{\rm inc}^{\rm Glob}(Q,\omega) + A_0(Q)\left(1-A_1(Q)\right)S_{\rm inc}^{\rm Glob}(Q,\omega)\otimes S_{\rm inc}^{\rm HJ}(Q,\omega) \\ & + \left(1-A_0(Q)\right)L^{\rm Conf}(Q,\omega). \end{aligned} \tag{10}$$

Since τ_2 is expected to be long compared to the energy resolution of the present experiment, we can further simplify the expression above and write

$$A_0(Q)A_1(Q)S_{\rm inc}^{\rm Glob}(Q,\omega) \approx A_0(Q)A_1(Q)\delta(\omega). \tag{11}$$

The QENS cross section is then given by

$$\begin{aligned} \frac{\partial^2\sigma}{\partial\Omega\partial\omega} = {} & \frac{k}{k_0}\frac{\sigma_{\rm inc}}{4\pi}\mathrm{e}^{-Q^2\langle u^2\rangle/3}\big[B_0(Q)\delta(\omega) + B_1(Q)S_{\rm inc}^{\rm Glob}(Q,\omega)\otimes S_{\rm inc}^{\rm HJ}(Q,\omega) \\ & + B_2(Q)L^{\rm Conf}(Q,\omega)\big] \end{aligned} \tag{12}$$

where $\sigma_{\rm inc}$ is the average incoherent cross section of the nuclei in the sample and the exponential factor is the Debye–Waller factor accounting for the loss of QENS intensity to fast motions described by a mean-square amplitude $\langle u^2\rangle$. For the sake of clarity, the detailed balance factor is not explicitly specified in equation (12) but was taken into account in the model fits. The model scattering function was also convoluted with the resolution function of the spectrometer.

3. Experimental details

We have applied the model described in section 2.2 to a QENS measurement of the dynamics of PEO melt on the QENS instrument [11] at the Intense Pulsed Neutron Source. The scattering function $S(Q,\omega)$ was measured over a Q range of 0.3–2.6 $\mathrm{Å}^{-1}$, with an average energy resolution of 80 μeV. Owing to the large incoherent neutron scattering cross section of the ^{1}H nucleus and the abundance of this element in polymeric samples, QENS measurements give a global view of the fast (ps–ns time scale), local (∼0.1 nm distance scale) dynamics of the polymer in terms of the uncorrelated motions of its hydrogen atoms [9]. The sample consisted of a film, 0.2 ± 0.05 mm thick, prepared by melting hydrogenous PEO (Aldrich, $T_{\rm m} \approx 62\,^{\circ}$C, $M_{\rm W} \approx 100\,000$, i.e. well above the entanglement threshold of ∼3600) under dry air at 95 °C onto a Teflon-coated plate. QENS spectra were recorded at a sample temperature of 100 °C. The scattering from an empty cell was subtracted and the signal was normalized with respect to a vanadium standard.

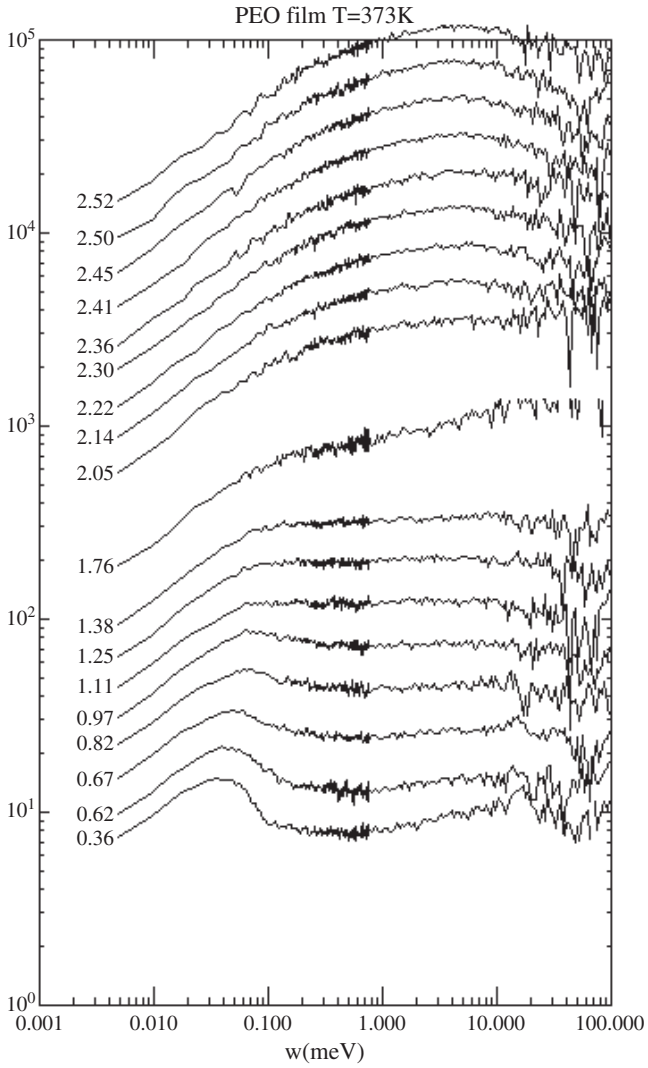

Figure 1. Susceptibility function, $\chi''(Q, \omega)$ versus ω, for PEO melt at 100 °C. The value of Q_0, the scattering vector corresponding to elastic scattering for a particular detector group, is indicated at the left of each curve.

4. Results

4.1. Susceptibility spectra

To highlight the various dynamical processes involved, the results are presented in figure 1 for the 17 detector groups in terms of the susceptibility function $\chi''(Q, \omega)$. A relaxation mechanism with characteristic time τ will appear as a quasi-elastic peak of HWHM $E \approx h/2\pi\tau$ in $S(Q, \omega)$ and as a band with a maximum at $E \approx h/2\pi\tau$ in $\chi''(Q, \omega)$. Two dynamical regions can be identified. A low-energy dispersive band ($E \approx 0.4$ meV at $Q_0 = 0.36$ Å^{-1}) merges at higher Q with a non-dispersive band ($E \approx 5$ meV), giving rise above 1.75 Å^{-1} to a broad peak. Smith *et al* [12] have observed a similar broad excitation in QENS spectra

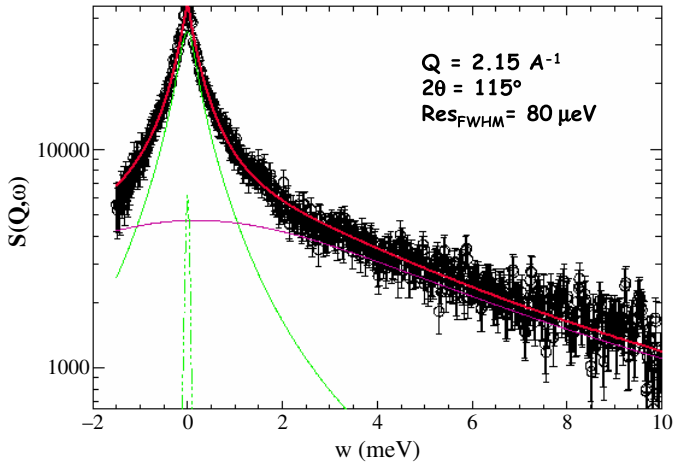

Figure 2. Semi-logarithmic plot of the quasi-elastic signal of bulk PEO at 2.15 Å^{-1} at $T = 373$ K showing the fit of equation (12) (full red line) along with the three components: green dotted, narrow (green) solid, and broad (purple) solid lines for the first, second, and third terms, respectively.

from a polyethylene melt. By means of a parallel molecular dynamics simulation, they were able to show that this band can be decomposed into two contributions: at high Q (1.8 Å^{-1}) the excitation is due almost entirely to librational movements, while at small Q (0.8 Å^{-1}) an additional contribution comes from conformational transitions along the polymer backbone from one rotational isomeric state to another.

4.2. Analysis of the QENS signal

The functional form given by equation (12) was fitted for each detector separately. It accounts very well for the QENS spectra of bulk PEO at 373 K over the energy range from -2 meV to $+10$ meV (neutron energy loss)—see figure 2. A key point of this study is that, in contrast to NMR, neutron scattering experiments access the Q dependence of the correlation times and hence provide spatial information. Over the Q range of this experiment, the three correlation times deduced from the fit of equation (12) are separated by at least one order of magnitude (figure 3(a)). This validates *a posteriori* the assumption made about the independence of the three dynamical contributions to the model and also the approximations of equations (8) and (9).

The relaxation time for the conformational motions, τ_0, is found to be relatively short and independent of Q, as expected for a reorientational and therefore non-dispersive motion. It accounts for the rather broad Lorentzian line with HWHM around 5 meV in figure 1. A similar short correlation time, corresponding to an energy HWHM of 5 meV, has been reported previously in PEO melts [13]. $A_0(Q)$, easily extracted from B_1, B_2 and B_3 (figure 3(b)), provides geometrical information. As shown in figure 5(a), $A_0(Q)$ is almost constant above 2.0 Å^{-1} at an unusually high value of 0.42. Such a large EISF value at high Q is consistent only with a jump motion between two distinct sites, as in equation (3). The best agreement is found for $d_j \sim 2.1$ Å.

The correlation time τ_1 follows a Q^{-2} power dependence characteristic of a translational diffusive motion. From a linear fit of the curve τ_1 versus Q^{-2} we obtain a value for the diffusion coefficient $D = 1.78 \times 10^{-9}$ $\text{m}^2\,\text{s}^{-1}$. The present QENS measurements access

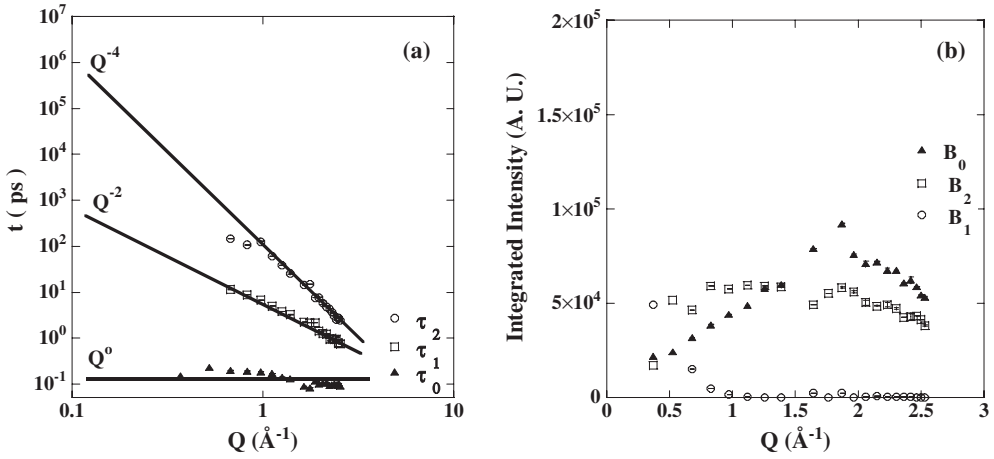

Figure 3. (a) Correlation times derived from the fits of equation (5) to the QENS data; the straight lines indicate the approximate power-law behaviours. (b) Intensities $B_0(Q)$, $B_1(Q)$ and $B_2(Q)$ derived from the fits.

proton average dynamics on a length scale of the order of a covalent bond. The covalent bonds are rigid on the meV energy scale, so any proton translational diffusion coefficient can be associated directly with that of a single monomer considered as a rigid body. Defining a monomeric friction coefficient $\xi_0 = k_B T/D$, where k_B is the Boltzmann constant, we find $\xi_0 = 2.89 \times 10^{-12}$ N s m^{-1}.

The monomeric friction coefficient plays a central role in polymer dynamics and is present in all theoretical expressions describing polymer dynamics from the short-time semi-local scale (Rouse dynamics) up to the long-time global scale (reptation). Using a segment length $\sigma = 4$ Å, [1] the above value for ξ_0 leads to the elementary Rouse relaxation rate $W = 3k_B T/(\xi_0 * \sigma^2) = 1.11 \times 10^{10}$ s^{-1} at 373 K, in agreement with recent PEO melt data in the nanosecond time range [14]. The parameter ξ_0 can be used to estimate at longer times, even in the reptation situation, the single-chain centre-of-mass diffusion coefficient $D_{cm} = M_m k_B T M_e/(3\xi_0 M^2)$ (for polymer molecular weight $M >$ the entanglement mass M_e, as here), where M_m is the monomer molecular weight. We find $D_{cm} = 9.4 \times 10^{-15}$ m^2 s^{-1}, in good agreement with pulsed field gradient NMR data on PEO melt at 373 K by Appel and Fleischer [15] (see figure 4).

The Q dependence of τ_2 is consistent with a Q^{-4} power law. Such behaviour is frequently observed in polymer melt dynamics analyzed on the basis of stretched exponential functions, where the stretching parameter β is found to be ∼0.5. In those cases, τ^β goes as Q^{-2} and thus satisfies the Gaussian approximation. As expected, the numerical values of τ_2 extracted from the fits are long compared to the resolution of the instrument used here, validating the approximation of equation (11).

The values derived for $A_1(Q)$ are shown in figure 5(b). They are relatively low over most of the Q range of the present measurements and can be better accessed with higher energy resolution at low Q. We have re-analyzed high-resolution (15 μeV) data from hydrogenated PEO ($M_W = 40,000$) measured at 75 °C on the IRIS instrument at ISIS [7], fitting them with an expression similar to equation (12). Due to the higher resolution, limited Q range ($Q_{max} = 1.7$ Å^{-1}) and modest dynamical range (±100 μeV), the jump diffusion related parameters were fixed at the values measured in the present work at IPNS, i.e., $\tau_0 = 0.15$ ps and

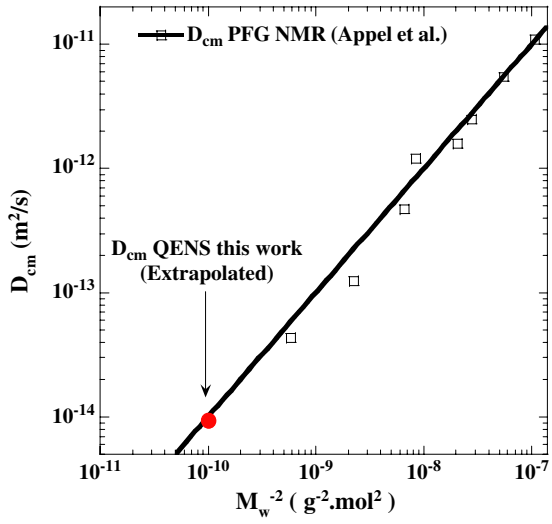

Figure 4. Molecular weight dependence of the PEO chain centre-of-mass self-diffusion coefficient $D_{\rm cm}$ (PFG NMR data from [15]). The point extrapolated using the Doi–Edwards theory with a monomeric friction coefficient $\xi_0 = 2.89 \times 10^{-12}$ N s cm^{-1}, derived from the Q^2 dependence of τ_1, is indicated by an arrow.

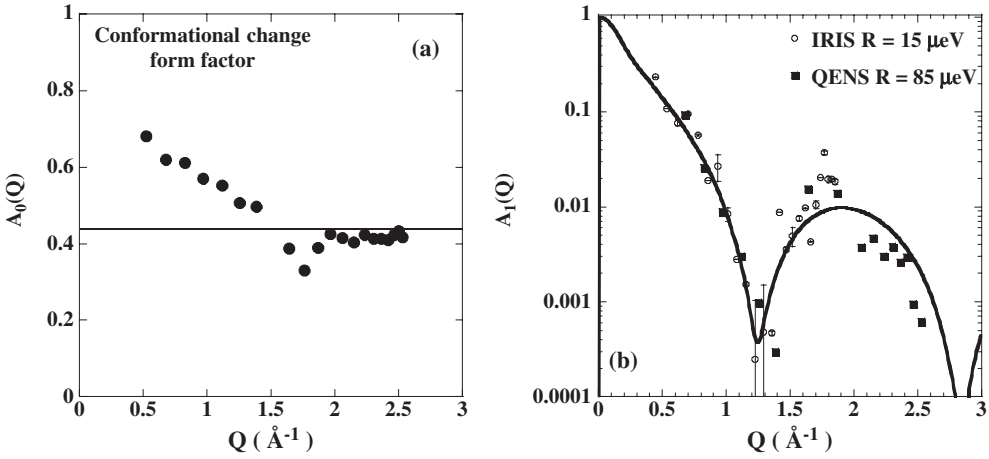

Figure 5. (a) $A_0(Q)$, form factor (EISF) for conformational changes, extracted from equation (12) and the measured intensities B_1, B_2 and B_3 (see also figure 4). The full horizontal line indicates the level $(1 - a)$ of the weighting factor balancing short and long correlation time contributions to ^{13}C spin–lattice relaxation NMR spectral density (see equation (13) and [18]). (b) Semi-log plot of $A_1(Q)$ versus Q deduced from the fit of equation (12) to IRIS higher-resolution, low-Q data (open circles) and QENS low-resolution, high-Q data (black squares). The full line represents the form factor of a cylinder of 2.0 Å radius and 26 Å length.

$d_j \sim 2.1$ Å. The values of $A_1(Q)$ measured on the two instruments are in good agreement and are well accounted for by the EISF of a cylinder of 2.0 Å radius and 26 Å length (figure 5(b)).

The present analysis of QENS data for PEO melt can be combined with the results of a molecular dynamics simulation study of conformational changes in PEO [10] to obtain a detailed insight of the melt dynamics. Due to fast $g^{\pm}tt \leftrightarrow ttg^{\pm}$ and $ttt \leftrightarrow g^{\pm}tg^{\pm}$

conformational rearrangements of the chain structure, a hydrogen atom experiences jump diffusion between two sites separated by a distance of the order of 2 Å (from the form factor $A_0(Q)$). Our results show that the jump between adjacent sites (rotation of a chain segment) is coupled to a translational motion ($\tau_1 \sim Q^{-2}$) giving rise to an overall helical jump movement. Due to the damping effects of the neighbouring chains and/or topological constraints (e.g., entanglements), the translational movement of the whole chain is confined within a cylinder that is a few nm long (form factor $A_1(Q)$).

4.3. Comparison with NMR relaxation data

Detailed molecular dynamics can be also assessed by NMR. Hall and Helfand (HH) [16] derived a bimodal autocorrelation function to describe damped conformational changes along a polymer chain. Subsequently, Dejean de la Batie *et al* (DLM) [17] showed that this autocorrelation function could not account for the high value of the spin–lattice relaxation time T_1 observed in ^{13}C spin–lattice relaxation time experiments [18]. To explain their data, they complemented the HH model with an additional fast, small-amplitude anisotropic motion that they identified with librations of C–H vectors:

$$G(t) = (1-a)\mathrm{e}^{-t/\tau_1}\mathrm{e}^{-t/\tau_2} I_0(t/\tau_1) + a\mathrm{e}^{-t/\tau_0}. \tag{13}$$

In the first term, following [16], τ_1 is the correlation time associated with the conformational jumps responsible for orientational diffusion along the polymer chain, while τ_2 represents a damping mechanism consisting of either non-propagating isolated motions or distortions of the chain with respect to its stable local conformation. The fast relaxation τ_0 corresponds to the correlation time of librations of C–H vectors inside a cone of half-angle θ, and a is a geometrical factor depending on $\cos\theta$. In the case of PEO with $M = 9200$ g mol^{-1} at 373 K, Dejean de la Batie *et al* [18] report $\tau_1 \approx 4$ ps, $\tau_1/\tau_0 = 200$, $\tau_1/\tau_2 = 200$, and $a = 0.56$, corresponding to the libration of a CH bond in a cone of half-angle $\theta = 40°$.

There is clearly a formal similarity between the DLM model and that proposed here. For the sake of comparison, we express the latter in the variables Q and t:

$$I(Q,t) = A_0(Q)A_1(Q) + A_0(Q)(1-A_1(Q))\mathrm{e}^{-t/\tau_1}\mathrm{e}^{-t/\tau_2} I_0(t/\tau_1) + (1-A_0(Q))\mathrm{e}^{-t/\tau_0}. \tag{14}$$

As is immediately apparent from a comparison of equations (13) and (14) and as stated in the introduction, the presence of the variable Q makes it hard to compare directly models derived for QENS and NMR data. Based on the simple qualitative argument that NMR accesses local, atomic-scale dynamics, we can take the lower end of the equivalent Q range to be around 2 Å^{-1}, so that $2\pi/Q_{\min} \sim 3$ Å is on the order of two or three covalent bonds.

As shown in figure 5(a), the NMR value of $a = 0.56$ (equation (13)) agrees with the high-Q limit of the QENS form factor, $[1 - A_0(Q)] = 0.56$. Moreover, at high Q, $A_1(Q) \sim 0$ and the elastic term disappears, so that equation (14) reduces exactly to equation (13).

Despite this formal similarity, our results lead to a different interpretation of the PEO dynamics from that proposed by HH and DLM as an orientational propagation of conformational changes along the polymer chain. Such a collective excitation would not induce any translational diffusion of the protons and so could not account for the Q^{-2} dependence of τ_1 as measured on our hydrogenated sample. Moreover, our result show that the fast relaxation time τ_0 is mainly related to two-site jump conformational changes as opposed to CH torsional librations within a cone. From the Q dependence of the total scattered intensity loss (the Debye–Waller factor in equation (12)), we estimate the mean-square displacement due to correlation times much shorter than τ_0 to be $\langle u^2\rangle/3 = 0.13$ Å^{-2}. This value corresponds to

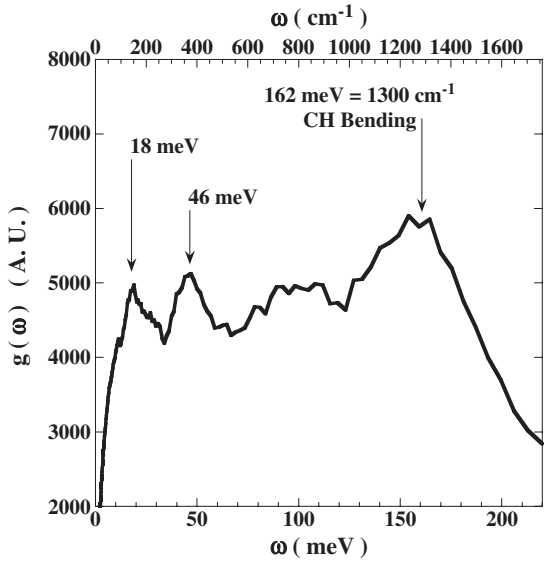

Figure 6. Vibrational density of states $g(\omega)$ of PEO melt at 373 K.

a libration of a C–H bond in a cone of half-angle $\theta = 35°$, in relatively good agreement with the value proposed by DLM. From an analysis of the vibrational density of states (figure 6), it appears that C–H vectors are likely to experience a torsional mode with a libration energy of ∼18 meV.

Two-dimensional (2D) NMR exchange studies of the chain dynamics in polymer melts (close to the glass transition) show that the geometry of the chain motion in melts is ill-defined and involves a combination of rotational-diffusion-like motions through 'small angles' below 10° and large angle jumps through 10° or more [19]. As opposed to the present work (melt at high temperature), no well-defined jump between two sites is observed by multi-dimensional NMR in the melt at low temperature.

A fit of the experimental EISF, figure 5(a), with equation (3) is far from satisfactory so, even as sensed by neutrons, the jump motion is actually not really a pure two-site jump motion. But since, at the short time scale with which we are dealing, the high-Q limit of the EISF is well defined (EISF $\approx$ 0.5), it seems that the disagreement is related to an ill-defined jump length rather than an ill-defined number of sites.

The 0.5 limit of the EISF at high Q is significant, since it is almost exactly the weighting factor that balances the two terms of equation (13) (DLM model) and equation (14) (model proposed here). This agreement is interesting, because it refers to results obtained by two independent techniques probing short-time dynamics (tens of ps in the neutron case and ns in that of C13 spin lattice relaxation NMR) on the same system (PEO melt) at the same relatively high temperature above T_g. The apparent discrepancy about the existence of two-site jumps between the neutron and multi-dimensional NMR results could be due to (i) the different temperatures that the system is probed at (far above T_g and around T_g, respectively) or (ii) the fact that, in neutron scattering, dynamical modes with higher spatial extent make a larger contribution to the signal.

As emphasized by Moe *et al* [20], the DLM model in the form given in equation (13) does not appear to be a suitable model to fit NMR data from polymer melts. These authors find that

the best description is obtained with a sum of a fast component and a stretched exponential term. Such a model has in fact been shown by Triolo *et al* [13] to be useful in fitting QENS data from a PEO melt. Nevertheless, in order to get a perfect fit to these data, Triolo *et al* had to take into account a small elastic contribution. The model proposed here, equation (12), gives a physical basis to all correlation times involved, together with an assignment of this elastic contribution to localization of the polymer chain within a cylinder at short (ps) times. We note that the chain is expected to leave this confinement volume at times longer than a few tens of ps, so that the elastic contribution given in equations (11) and (12) is likely to appear broadened at higher energy resolution.

5. Conclusions

The analysis of QENS data from a polymer melt proposed in this work leads to an appealing physical interpretation of local polymer dynamics. We are able to determine a monomeric friction coefficient that adequately describes, in the framework of the Doi–Edwards theory, the long-time polymer behaviour in the Rouse (probed by neutron spin-echo measurements) and reptation (probed by PFG NMR) regimes. This could be a route for estimating the monomeric friction coefficient, and hence rheological properties, in physical environments such as nano-confinement, where rheological measurements are impossible. We show for the first time that high-Q (>0.2 Å^{-1}) QENS data are consistent with theoretical (Rouse and reptation) concepts usually expected to fail in this regime, and that the DLM model derived from NMR results is a special case of the model proposed here, corresponding to a high-Q limit. However, the two models have very different physical interpretations. It would be interesting to test the model proposed here with T_1 NMR data on PEO melt.

Acknowledgments

The authors would like to thank R Connatser for continued assistance during the neutron scattering experiments. This work was supported by the Office of Science, US Department of Energy, under Contract W-31-109-ENG-38, the Commissariat à l'Energie Atomique (CEA, France), the Centre National de la Recherche Scientifique (CNRS, France), and the University of Orléans. The authors acknowledge fruitful discussion with Professor H W Spiess about the detailed dynamical modes, as seen by NMR, that come into play in a polymer melt.

References

[1] Ferry J D 1980 *Viscoelastic Properties of Polymers* (New-York: Wiley)
[2] Rouse P E 1953 *J. Chem. Phys.* **21** 1272
[3] de Gennes P-G 1967 *Physics* **3** 37
[4] Schmidt-Rohr K and Spiess H W 1994 *Multidimensional Solid-state NMR and Polymer* (New-York: Academic)
[5] Richter D 2000 *Physica* B **276–278** 22
[6] Harnau L, Winkler R G and Reineker P 1997 *J. Chem. Phys.* **106** 2469
[7] Mao G, Fernandez Perea R, Howells W S, Price D L and Saboungi M-L 2000 *Nature* **405** 163
[8] Saboungi M-L, Price D L, Mao G, Fernandez-Perea R, Borodin O, Smith G G, Armand M and Howells W S 2002 *Solid State Ion.* **147** 225
[9] Bée M 1988 *Quasielastic Neutron Scattering: Principles and Applications in Solid-state Chemistry, Biology and Material Science* (Bristol: Hilger)
[10] Borodin O and Smith G D 2000 *Macromolecules* **33** 2273

[11] Connatser R W, Belch H, Jirik L, Leach D J, Trouw F R, Zanotti J-M, Ren Y, Crawford R K, Carpenter J M, Price D L, Loong C-K, Hodges J P and Herwig K W 2003 *Proc. ICANS-XVI, 16th Meeting of the Int. Collaboration on Advanced Neutron Sources (Düsseldorf-Neuss, Germany, May 2003)*
[12] Smith G D, Paul W, Monkenbusch M and Richter D 2000 *Chem. Phys.* **261** 61
[13] Triolo A, Arrighi V, Triolo R, Passerini S, Mastragostino M, Lechner R E, Ferguson R, Borodin O and Smith G D 2001 *Physica* B **301** 163
[14] Genix A-C, Arbe A, Alvarez F, Colmenero J, Willner L and Richter D 2005 *Phys. Rev.* E **72** 31808
[15] Appel M and Fleischer G 1993 *Macromolecules* **26** 5520
[16] Hall C K and Helfand E 1982 *J. Chem. Phys.* **77** 3275
[17] Dejean de la Batie R, Laupretre F and Monnerie L 1988 *Macromolecules* **21** 2045
[18] Dejean de la Batie R, Laupretre F and Monnerie L 1988 *Macromolecules* **21** 2052
[19] Tracht U, Heuer A and Spiess H W 1999 *J. Chem. Phys.* **111** 3720
[20] Moe N E, Qiu X H and Ediger M D 2000 *Macromolecules* **33** 2145